

Microtubule-stabilizing properties of the avocado-derived toxins (+)-(*R*)-persin and (+)-(*R*)-tetrahydropersin in cancer cells and activity of related synthetic analogs

Jessica J. Field^{1,2} · Arun Kanakkanthara^{1,3} · Darby G. Brooke^{4,5} · Saptarshi Sinha¹ · Sushila D. Pillai¹ · William A. Denny^{5,6} · Alison J. Butt⁷ · John H. Miller¹

Received: 10 January 2016 / Accepted: 7 March 2016 / Published online: 12 March 2016
© Springer Science+Business Media New York 2016

Summary The avocado toxin (+)-*R*-persin (persin) is active at low micromolar concentrations against breast cancer cells and synergizes with the estrogen receptor modulator 4-hydroxytamoxifen. Previous studies in the estrogen receptor-positive breast cancer cell line MCF-7 indicate that persin acts as a microtubule-stabilizing agent. In the present study, we further characterize the properties of persin and several new synthetic analogues in human ovarian cancer cells. Persin and tetrahydropersin cause G₂M cell cycle arrest and increase intracellular microtubule polymerization. One analog (4-nitrophenyl)-deshydroxyersin prevents cell proliferation and blocks cells in G₁ of the cell cycle rather than G₂M, suggesting an additional mode of action of these compounds independent of microtubules. Persin can synergize with other microtubule-stabilizing agents, and is

active against cancer cells that overexpress the P-glycoprotein drug efflux pump. Evidence from Flutax-1 competition experiments suggests that while the persin binding site on β-tubulin overlaps the classical taxoid site where paclitaxel and epothilone bind, persin retains activity in cell lines with single amino acid mutations that affect these other taxoid site ligands. This implies the existence of a unique binding location for persin at the taxoid site.

Keywords Cancer · Microtubule-stabilizing agent · Multidrug resistance · Persin · Tetrahydropersin · Synergy · Taxoid binding site · Peloruside · Flutax-1

Jessica Field and Arun Kanakkanthara contributed equally to the paper.

✉ John H. Miller
john.h.miller@vuw.ac.nz

Abbreviations

CI	Combination index
MDR	Multidrug resistance
MSA	Microtubule-stabilizing agent
P-gp	P-glycoprotein
T-persin	Tetrahydropersin

Introduction

The avocado cytotoxin, (+)-(*R*)-persin ((+)-(*R*)-(Z,Z)-1-(acetyloxy)-2-hydroxy-12,15-heneicosadien-4-one) (persin) (Fig. 1), a polyketide long-chain lipid similar to linoleic acid (Fig. 1), was first isolated and described forty years ago [1], with its absolute configuration confirmed twenty years later by stereoselective synthesis [2, 3]. Amongst other biological activities, it has been shown to have antifungal activity in unripe avocado fruit [4], to be a deterrent to insect feeding [5], and to be orally toxic to silkworm larvae [1]. Oelrichs et al. [2] additionally confirmed that persin, and its fully saturated analogue tetrahydropersin (T-persin) (Fig. 1), which also occurs naturally

- ¹ Centre for Biodiscovery, School of Biological Sciences, Victoria University of Wellington, PO Box 600, Wellington 6140, New Zealand
- ² Present address: Seattle Genetics, Bothell, WA 98021, USA
- ³ Present address: Department of Pediatric and Adolescent Medicine, Mayo Clinic, Rochester, MN 55905, USA
- ⁴ Present address: Cawthron Institute, Private Bag 2, Nelson, New Zealand
- ⁵ Auckland Cancer Society Research Centre, The University of Auckland, Auckland, New Zealand
- ⁶ Maurice Wilkins Centre, University of Auckland, Auckland, New Zealand
- ⁷ Cancer Research Program, Garvan Institute of Medical Research, St. Vincent's Hospital, Darlinghurst, New South Wales, Australia

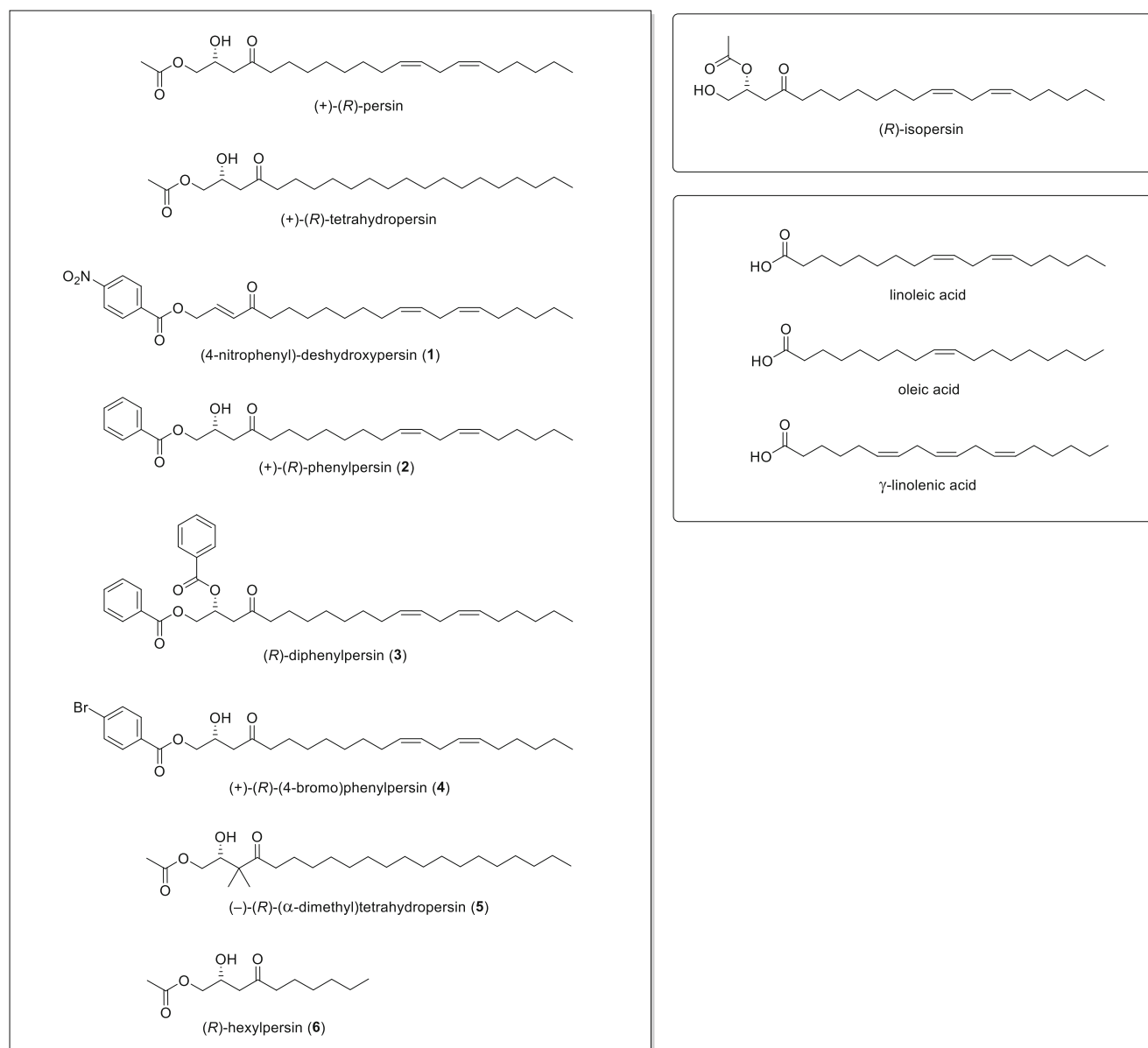


Fig. 1 Chemical structures of persin and selected synthetic analogs, and related unsaturated fatty acids

in the avocado plant [6], caused necrosis of the secretory epithelial cells in lactating mice, mirroring the reported effects of avocado leaf ingestion in other lactating livestock [7]. However, they found its unnatural (*S*)-isomer was inactive in this context. Polyunsaturated fatty acids are known to increase the sensitivity of breast cancer cells to chemotherapeutics such as paclitaxel [8], suggesting the possibility of using persin in combination therapy with this anticancer drug. Moreover, the targeting of the secretory epithelium of the mammary gland by persin suggests it may have a role in the treatment of breast cancer, and a number of studies have been carried out to test this hypothesis [9–12].

Persin was shown to arrest cells in G_2M of the cell cycle and induce microtubule stabilization in MCF-7 estrogen receptor-positive breast cancer cells [9]. The action of persin,

however, is independent of the estrogen receptor, p53, and Bcl-2 status of the cells [9], and its induction of apoptosis is dependent on Bim (BH₃-only protein) expression [9]. Other compounds that target the microtubule, including microtubule-stabilising agents (MSAs) such as the Pacific yew tree-derived paclitaxel and its semi-synthetic analog docetaxel, have proven to be successful chemotherapeutic drugs [13]. Treatment of cells with paclitaxel results in the phosphorylation and deactivation of Bcl-2, a protein that promotes cell survival in cancer cells, thus leading to cell death by apoptosis [14]. Polyunsaturated acids, such as γ-linolenic acid (Fig. 1), can directly modulate estrogen receptor sensitivity to circulating hormones, possibly by down-regulation of the receptor [10]. These drugs have successfully progressed into clinical trials for estrogen receptor-positive breast cancer, in

combination with 4-hydroxytamoxifen, the active metabolite of tamoxifen and an estrogen receptor antagonist [15]. Persin, similar to γ -linolenic acid, is also effective against estrogen receptor-negative breast cancer cells that are resistant to tamoxifen [10, 11]. The mechanism of action of persin in such cells appears to involve increased ceramide signalling of Bim through a JNK/cJun pathway, leading to mitochondrial release of cytochrome c and apoptosis [10]. Interestingly, as Bim is a sensor of microtubule integrity, it binds to the dynein motor protein, and thus also plays a key role in MSA-induced apoptosis [16].

The inflammatory caspase, caspase-4, also appears to be involved in the action of persin, as shown by the fact that siRNA knockdown of caspase-4 prevents persin-induced apoptosis [11]. The specific targeting of cancer cells over normal cells by persin or persin extracts has been demonstrated in breast cancer cells [10], oral epithelial cells [17, 18], and lymphoblastic leukemic T-cells (Jurkat cells) [12, 19]. The dependence of persin on the inflammatory caspase-4 [11] may explain part of its cancerous T-cell-targeting ability, since caspase-4 mediates the induction of apoptosis by endoplasmic reticulum stress, and there are links between inflammation and cancer [20]. Reactive oxygen species and endoplasmic reticulum stress markers also appear to be involved in the mode of action of persin [11, 12, 17, 18].

Fine-tuning of persin-based analog design requires a detailed structure-activity analysis. Persin comprises a β -hydroxy ketone system, flanked by an acetate on one side and a long-chain unsaturated fatty acid on the other. Isopersin (Fig. 1), in which these moieties are in opposite positions, lacks biological activity [21], suggesting that the relative location of these moieties is essential for the biological activity of persin, or its metabolism to an active form. Brooke et al. [22] reported structure-activity studies of persin, T-persin, and nine synthetic analogs, six of which showed cytotoxic activity in various cell lines, but with slightly reduced potency compared to the parent compound. The IC_{50} for inhibition of cell proliferation of MCF-7 breast cancer cells was 15 μ M and 17 μ M for persin and T-persin, respectively, and ranged from 20–29 μ M for the four synthetic analogs that showed activity [22].

The aim of the present investigation was to confirm the microtubule-stabilizing activity of persin, T-persin, and six of the analogs originally synthesized in our laboratory (compounds 1–6, Fig. 1) in two non-breast cancer cell lines. Given the unusual structure of persin, such confirmation would exemplify its being a novel MSA chemotype. As it is not known whether the microtubule-stabilizing effects of persin are due to its interaction with tubulin or with microtubules themselves [9], we examined the ability of persin and two of its analogs to polymerize tubulin inside cells and to cause G₂M arrest, a characteristic property of compounds that target the microtubule. In addition, we examined

the activity of these compounds in cells overexpressing the P-glycoprotein (P-gp) drug efflux pump, a major contributor to MDR. We also looked at the effect of mutations in the two recognized binding sites for MSAs on persin activity, namely the taxoid site where paclitaxel and epothilones bind [23] and the laulimalide/peloruside binding site [24]. Lastly, we determined if persin and T-persin could synergize with other MSAs that bind to the two known sites on β -tubulin, since, in theory, such synergy should not occur if two ligands compete for the same site. We hypothesized that the findings from these investigations, taken together, would provide insights into whether persin occupies a novel binding site on tubulin.

Materials and methods

Compounds

Persin, T-persin, and analogs 1–6 were prepared as described previously [22]. Paclitaxel was purchased from Sigma-Aldrich Corporation (St. Louis, MO), and ixabepilone (Ixempra) was purchased from Bristol-Myers Squibb (New York, NY). Flutax-1 (7-O-[N-(4-fluoresceincarbonyl)-L-alanyl]-paclitaxel) was purchased from Pharmaco (NZ) Ltd. Peloruside A was isolated by Dr Peter Northcote and Dr Jonathan Singh, School of Chemical and Physical Sciences, Victoria University of Wellington from the marine sponge *Mycale hentscheli* (New Zealand) as previously described [25]. All compounds were estimated by ¹H NMR and TLC analysis as being >90–95% pure and were stored at -80°C as 1 mM stock solutions in absolute ethanol or DMSO.

Cell culture and MTT assay

Cells were cultured in a humidified 5% CO₂/air atmosphere at 37°C as previously described [26], using RPMI-1640 medium (Life Technologies, Australia) supplemented with 10% fetal bovine serum (Hyclone Laboratories, Logan, UT) and Pen-Strep (Life Technologies). For the ovarian carcinoma cell lines (1A9, A2780, A2780AD, PTX-10, PTX-22, A8, B10, R1, L4) and breast cancer cell lines (MCF-7, MDA-MB-231), 0.25 U/mL insulin (Sigma-Aldrich Corporation, St. Louis, MO) was also added to the medium. The MCF-7 cell line and the β -tubulin mutant 1A9 cell lines were a kind gift of Dr Paraskevi Giannakakou, Weill Medical College, Cornell University. The MDA-MB-231 cell line was a kind gift of Dr Euphemia Leung, University of Auckland, NZ. All other cell lines were obtained as previously described [26]. The effects of persin and its analogs on cell growth were assessed using an MTT (3-(4,5-dimethylthiazol-2-yl)-2,5-diphenyltetrazolium bromide) cell proliferation assay, as previously described [27]. In brief, cells were seeded into 96-well plates at a concentration of 1×10^4 cells per well,

and after treatment with test compounds for four days (two days for HL-60 cells), MTT tetrazolium dye (5 mg/mL) was added to the wells, and the resulting blue formazan crystals were dissolved in a mixture of 10% sodium dodecyl sulfate and 45% dimethylformamide at pH 5.5. The absorbance of the resulting solution at 570 nm was measured in a multilabel plate reader (EnVision®, PerkinElmer, Waltham, MA).

Flow cytometry

Cell cycle analysis was carried out by flow cytometry using a FACSCanto™ II with Diva software (Becton Dickinson Biosciences, Sparks, MD). Scan data were analyzed using FlowJo 7 software (v10.0.4; Tree Star, Ashland, OR). 1A9 cells were plated in 24-well plates at 1×10^5 cells/well and allowed to attach overnight. Cells were then treated with test compounds for 16 h in a CO₂/air incubator at 37°C. The cells were then resuspended in staining solution (0.05 mg/mL propidium iodide, 0.1% sodium citrate, 0.1% Triton-X100) with RNase (100 µg/mL) and incubated in the dark for 30 min, before assessing the DNA content of 10,000 cells in the FACSCanto™ II.

Cellular tubulin polymerization

The amount of soluble and polymerized tubulin in cells was assessed using an in situ cellular tubulin polymerization assay [26, 28]. In brief, 1A9 cells were treated with persin or one of its analogs for 16 h, and then lysed in a hypotonic buffer consisting of 1 mM MgCl₂, 2 mM EGTA, 1% Nonidet P-40, 50 mM Tris-HCl pH 6.8, and 10 µL/mL protease inhibitor cocktail (Sigma-Aldrich), and the soluble and polymerized tubulin separated at room temperature by centrifugation at 14,000 g for 10 min. The pellet (of polymerized tubulin) was resuspended in an equivalent volume of hypotonic buffer, and the samples were then electrophoresed and immunoblotted with an anti- α -tubulin rabbit primary antibody (1:1000, ab18251, Abcam) and a Cy5-conjugated goat anti-rabbit secondary antibody (1:2500, PA45011V, Amersham, GE Healthcare). The tubulin band densities were determined from a scan of the transfer membrane (Immobilon®-FL, Millipore Corp, Billerica, MA) on a Fujifilm FLA-5100 imaging system (Fuji Photo Film Co. Ltd., Japan), and scans were analyzed using ImageJ software (NIH).

Determination of combination index

The combination index (CI) for determining a synergistic interaction was calculated as previously described [29, 30] from the following equation: $CI = D_1/Dx_1 + D_2/Dx_2$ in which D_1 and D_2 are the concentrations of drug 1 and drug 2 that when given in combination give the same response as drug 1 alone (Dx_1) and drug 2 alone (Dx_2). A CI value <1.0 indicates

synergy, a CI value equal to 1.0 indicates additivity, and a CI value >1.0 indicates antagonism. It is generally accepted that a CI value must be ≤ 0.8 to indicate biologically significant synergy.

Flutax competition assay

A Flutax-1 competitive binding experiment was carried out with persin, following the method of Field et al. [31]. HL-60 promyelocytic leukemic cells were seeded into wells of a 24-well plate at 2×10^5 cells/well in 0.5 mL RPMI-1640 medium containing 10% fetal bovine serum. The cells were treated with different MSAs and Flutax-1 for 16 h at 37°C. The MSA concentrations used were based on the compounds' respective IC₅₀ values and thus spanned the nM range for pacilitaxel and peloruside and the µM range for persin. Flutax-1 was used at concentrations of 50 or 200 nM. Following MSA treatment, 50 µL of cell suspension from each well was centrifuged at 180 g for 5 min onto a glass slide in a Cytospin®3 centrifuge (Thermo Shandon, UK). A coverslip was mounted onto the slide with ProLong® Gold Antifade Reagent containing DAPI (Invitrogen, Eugene, OR), and the green fluorescent staining of Flutax-1 bound to microtubules and blue fluorescent staining of DAPI bound to DNA were imaged in an Olympus FluoView FV1000 confocal laser scanning microscope (inverted model IX81) using a 100× objective.

Data analysis

Statistical analysis of the data was conducted with Prism software (v5, GraphPad Software, San Diego, CA). Data sets were determined to be statistically different if $P \leq 0.05$.

Table 1 The average IC₅₀ values (µM) of persin and its analogs. Values are the mean \pm SEM of 3-7 independent biological replicates

	HL-60	1A9	MCF-7	MDA-MB-231
Persin	1.9 \pm 0.1	13.7 \pm 0.6	5.2 \pm 0.3	37.8 \pm 4.6
T-persin	0.6 \pm 0.03	4.1 \pm 0.4	2.0 \pm 0.3	48.8 \pm 5.2
1	4.0 \pm 0.1	18.9 \pm 1.3	23.3 \pm 1.6	18.4 \pm 4.6
2	2.6 \pm 0.4	19.4 \pm 2.2	-	-
3	7.5 \pm 0.2	21.2 \pm 1.8	-	-
4	5.8 \pm 0.1	34.1 \pm 5.3	-	-
5	28.4 \pm 0.5	47.6 \pm 3.5	-	-
6	22.8 \pm 1.0	124 \pm 20	-	-

HL-60: human promyelocytic leukaemia cells, 1A9: human ovarian carcinoma cells, MCF-7: human breast cancer cells, MDA-MB-231: human metastatic breast adenocarcinoma cells. Compounds 2–6 were not tested (-) in the MCF-7 and MDA-MB-231 cells

Results

Anti-proliferative activity of persin and its analogs

Persin, T-persin, and the synthetic analogs **1–6** (Fig. 1) were tested for cytotoxicity in the non-breast cancer cell lines HL-60 (human promyelocytic leukemic cells) and 1A9 (human ovarian carcinoma cells) using an MTT cell proliferation

assay. All analogs showed low μM inhibitory activity in both cell lines (Table 1), and **1** proved the most potent with IC_{50} values of 4 μM in HL-60 cells and 19 μM in 1A9 cells. Persin, T-persin, and **1** were then screened in MCF-7 breast cancer cells and in MDA-MB-231 metastatic breast cancer cells, with **1** proving the least active in MCF-7 cells but the most active in MDA-MB-231 cells. The IC_{50} values of **1–4** were comparable in both 1A9 and HL-60 cells, whereas **5** and **6** were less active

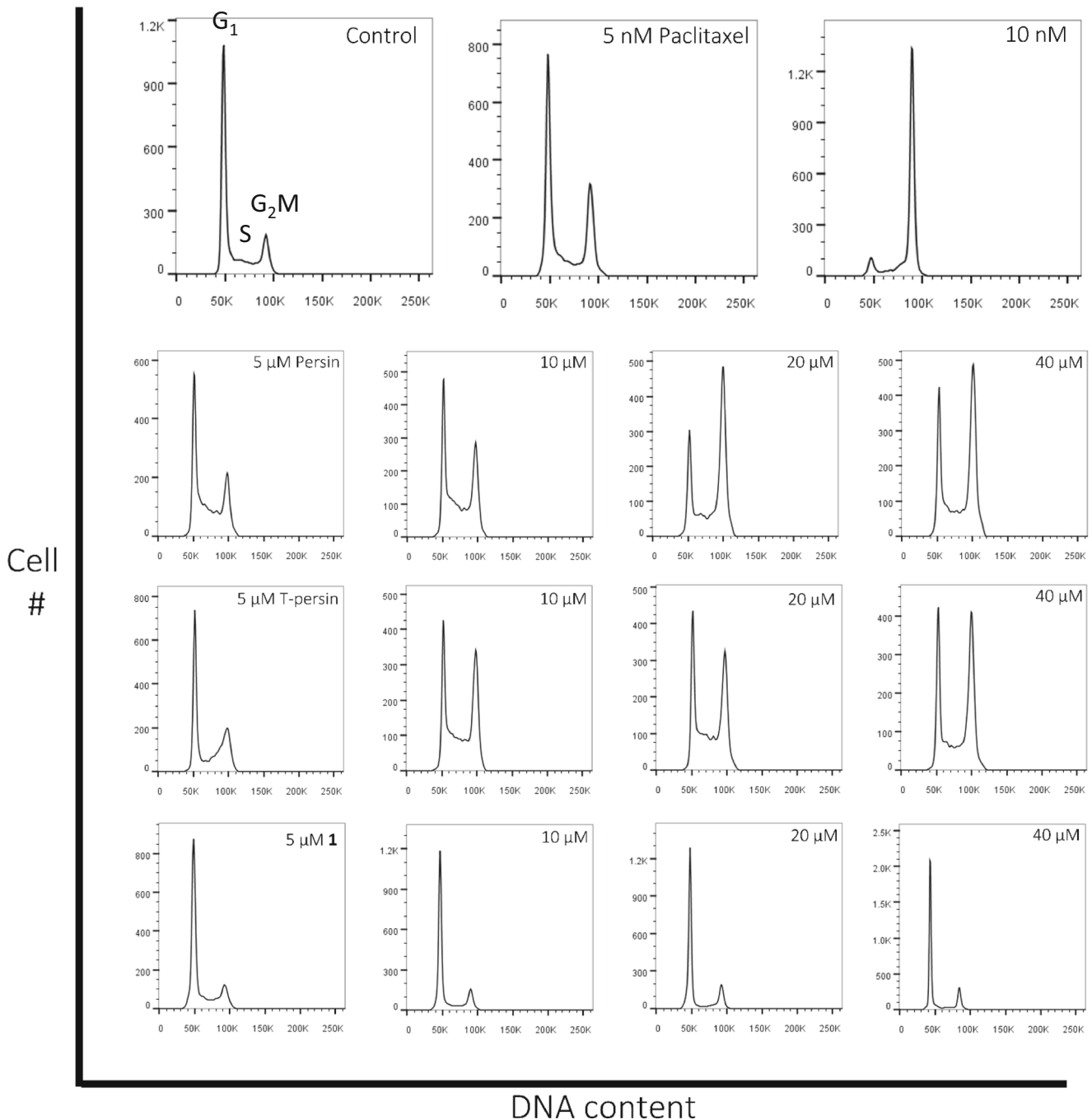


Fig. 2 Flow cytometry scans. The DNA content of 1A9 cells before (Control) and after 16 h treatment with persin, T-persin, or compound **1**, or with paclitaxel as an MSA positive control, was determined by flow

cytometry of propidium iodide-stained cells. The stage of the cell cycle, G_1 , S or G_2M , is identified on the Control scan only. See Table 2 for percentage of cells in each phase of the cell cycle

in these cell lines. Subsequent characterisation efforts were focused on delineating the other biological activities of persin, its natural analog (T-persin), and its most potent synthetic analog (compound **1**).

Cell cycle block by persin and two of its analogs

The effects of persin, T-persin, and compound **1** on progression of 1A9 cells through the cell cycle were analyzed by flow cytometry and compared to the effects of the known MSA paclitaxel in this cell line. Persin and T-persin caused a significant increase of cells in G₂M phase, variable changes in S phase cell levels, and a fall in the proportion of cells in G₁ phase, all of which were qualitatively similar to the effects of paclitaxel (Fig. 2; Table 2). In contrast, **1** had no effect on the proportion of cells in G₂M, but significantly increased the proportion of cells in G₁, redolent of the G₁ block generated by DNA replication inhibitors such as mimosine [32].

Effect of persin and two analogs on intracellular tubulin polymerization

Given the definitive G₂M block effected by persin and T-persin, the ability of these two compounds to induce tubulin polymerization in 1A9 cells was also tested. Both persin and T-persin increased the amount of polymerized tubulin in the cells (Fig. 3), verifying their microtubule-stabilizing activity as originally hypothesized by Butt et al. [9], based on these workers' analysis of the data they obtained for the action of persin in MCF-7 cells. **1** was also tested, and, consistent with its inability to effect a G₂M block, it also failed to induce significant tubulin polymerization in the cells (although **1** caused an increase from 17% polymerized tubulin in the control to 24–25% in the treated samples, the concentration-independence of this apparent increase is not consistent with a true polymerization effect). It is unclear why 17% polymerized tubulin is present in the 1A9 control cells for **1**: previous *in situ* polymerization experiments with 1A9 cells have yielded control percentage polymerized tubulin values of 0–4% [26, 33], more consistent with the values obtained for persin and T-persin than compound **1** in the present study (Fig. 3).

Activity of persin and two analogs in cell lines resistant to MSAs

The ovarian carcinoma cell lines A2780 (control phenotype) and A2780AD (MDR phenotype) were used to investigate the effect of overexpression of the P-gp drug efflux pump on the growth-inhibitory activity of persin and its analogs (Table 3). As expected, a 96-fold increase in the IC₅₀ of paclitaxel in the A2780AD (P-gp-overexpressing) cell line relative to its IC₅₀ in A2780 (low P-gp-expressing) cell line was observed that was consistent with the known susceptibility of this MSA to

P-gp-based drug efflux. In contrast, the IC₅₀ values of persin, T-persin, and **1** actually decreased slightly in P-gp-overexpressing A2780AD cells, relative to their IC₅₀ values in A2780 cells.

Combination treatment with paclitaxel or peloruside A

MSAs can have synergistic effects when given in combination, especially if they do not compete for the same binding site [29, 30]. Hence, peloruside A can synergize with paclitaxel or ixabepilone but not laulimalide, and paclitaxel is unable to synergize with most other taxoid site ligands, such as ixabepilone and docetaxel.

To investigate this, a range of concentration-combinations of persin and either paclitaxel or peloruside A was tested in 1A9 cells (Table 4). Significant synergy was seen for some combinations of these compounds, as demonstrated by combination index (CI) values <1 for 5 μM and 15 μM persin with 5 nM peloruside A (CI values of 0.5 and 0.6), and 10 μM persin with 5 nM and 2 nM paclitaxel (CI values of 0.6 and 0.7). Thus, only certain concentrations of persin could synergise with members of both classes of MSAs that bind to the two known binding sites on β-tubulin.

Investigation of the binding site of persin on tubulin

To locate a possible binding site on β-tubulin for persin and T-persin, the activity of these compounds in cells with single

Table 2 Cell cycle analysis

		G ₁	S	G ₂ /M
	Control	62.5 ± 0.9	18.3 ± 0.4	19.1 ± 0.5
Paclitaxel	5 nM	53.8 ± 0.0	13.6 ± 0.0	32.6 ± 0.0
	10 nM	11.7 ± 1.3	10.2 ± 1.4	78.2 ± 2.1
Persin	5 μM	41.9 ± 1.8	28.1 ± 1.0	29.9 ± 1.2
	10 μM	35.4 ± 1.6	22.2 ± 4.3	42.4 ± 5.7
	20 μM	24.8 ± 2.2	15.2 ± 1.5	60.0 ± 3.7
	40 μM	25.8 ± 2.0	13.8 ± 2.8	60.4 ± 4.7
T-persin	5 μM	47.3 ± 3.0	20.7 ± 5.2	32.0 ± 2.3
	10 μM	37.2 ± 1.5	28.6 ± 1.7	34.2 ± 2.3
	20 μM	32.0 ± 2.9	20.9 ± 3.5	47.1 ± 6.3
	40 μM	26.1 ± 2.8	15.5 ± 1.1	58.4 ± 3.9
Compound 1	5 μM	68.2 ± 1.0	14.4 ± 0.4	17.4 ± 0.8
	10 μM	70.9 ± 0.8	12.0 ± 1.0	17.1 ± 0.6
	20 μM	75.6 ± 9.1	9.1 ± 1.3	15.5 ± 0.5
	40 μM	73.7 ± 1.3	9.1 ± 0.5	17.2 ± 1.2

Human 1A9 ovarian carcinoma cells were treated with increasing concentrations of persin, tetrahydropersin (T-persin), compound **1**, or paclitaxel, and their DNA content subsequently examined by propidium iodide staining and flow cytometry. Data are presented as the mean % of cells ± SEM in each phase of the cell cycle. Data represent 3 or more independent experiments

amino acid point mutations at the two known β -tubulin binding sites of classical MSAs were examined to determine if the potencies of the compounds were affected by mutations at these binding sites (Table 5). All mutant tubulin cell lines were clones of the 1A9 ovarian carcinoma cell line, and at least two of the cell lines were known to have increased resistance to one or more of three MSAs as follows: paclitaxel (PTX-10; PTX-22; A8), epothilone (A8; B10), and peloruside A (1A9-R1; 1A9-L4) [28, 33–35]. The increased IC_{50} values (decreased potencies) of these MSAs in the resistant cell lines were 11-fold and 20-fold for paclitaxel (in PTX-10 and PTX-22, respectively), 12-fold and 15-fold for ixabepilone (azaepothilone B) (in A8 and B10, respectively) and 6-fold and 20-fold for peloruside A (in 1A9-R1 and 1A9-L4, respectively). However, the IC_{50} values of persin and T-persin were unchanged in these mutant cell lines, suggesting that on tubulin there exists either (a) a unique binding site for persin, or (b) a different binding site whose conformation is unaffected by the mutant amino acid.

Flutax-1 competition experiments (Fig. 4) indicated that excess persin was able to compete with Flutax-1 for its

Table 3 MDR susceptibility of persin and its analogs

	A2780	A2780AD	IC_{50} ratio (A2780/A2780AD)
Paclitaxel	3.0 ± 0.8	$288 \pm 66^*$	96
Persin	8.1 ± 1.1	6.1 ± 0.6	0.75
T-persin	8.1 ± 1.4	5.9 ± 1.2	0.73
Compound 1	13.7 ± 0.9	9.3 ± 0.7	0.68

Human A2780 and A2780AD (MDR phenotype) ovarian cancer cells were treated with paclitaxel, persin, T-persin, or **1**, and the IC_{50} (μ M) of each compound was determined from a subsequent MTT cell proliferation assay. $*P = 0.0002$, unpaired Student's *t*-test comparing IC_{50} values in A2780AD cells with A2780 control cells. The IC_{50} ratio = (IC_{50} in A2780AD)/(IC_{50} in A2780). Data are the average IC_{50} values in μ M \pm SEM (nM for paclitaxel) of 5 or more independent experiments

binding site (Fig. 4e,f), suggesting that the persin binding site is adjacent to or overlaps the taxoid site on β -tubulin, which prevents both compounds from binding simultaneously. As expected, excess paclitaxel displaced Flutax-1 from its binding site (Fig. 4d), while conversely, excess Flutax-1 could not be displaced by paclitaxel (Fig. 4c). Also as expected, peloruside, which binds to a different location on β -tubulin, distant from

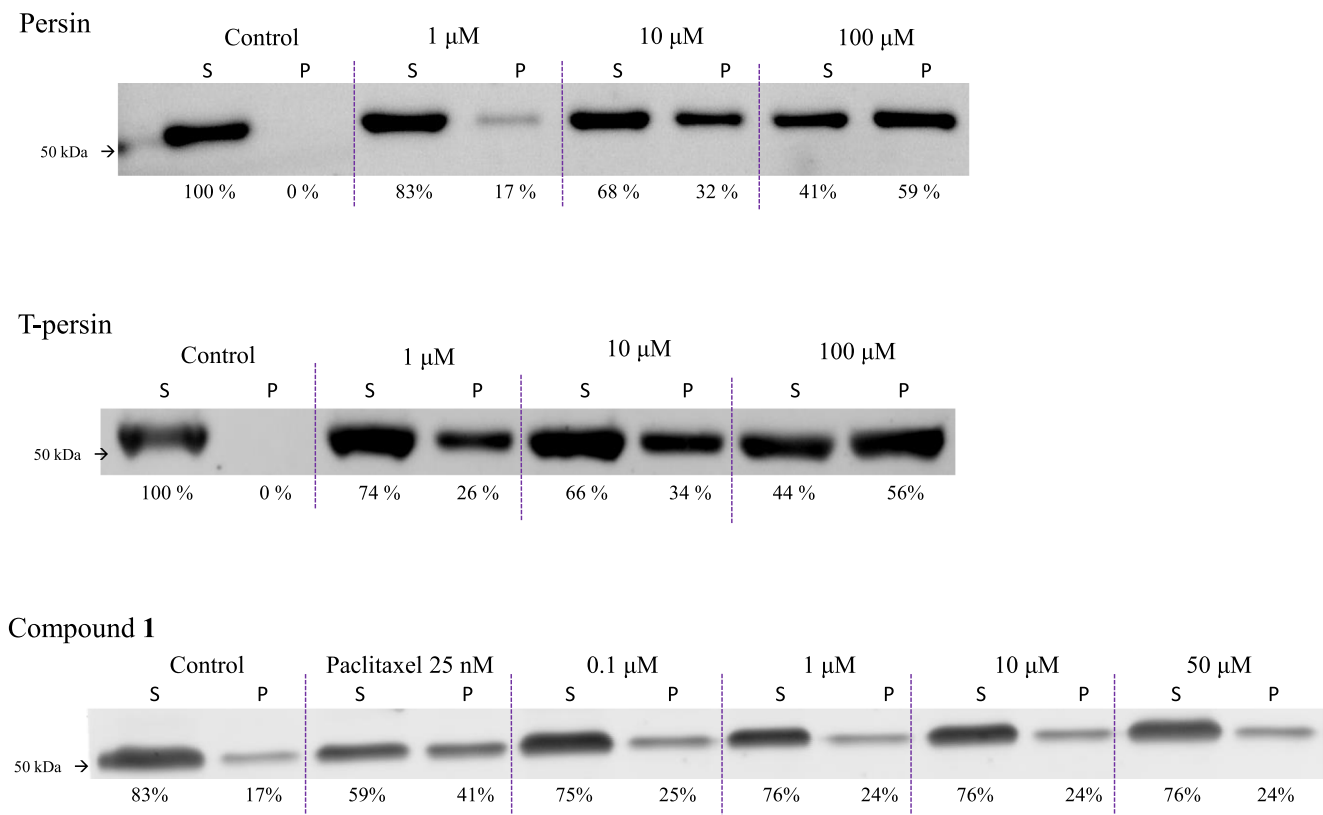


Fig. 3 Cellular tubulin polymerization. An in situ cellular assay was used to quantify drug-induced tubulin polymerization by SDS-PAGE electrophoresis of soluble (S) and pelleted (polymerized) (P) fractions of centrifuged cell lysates. 1A9 cells were treated for 16 hours with either persin, T-persin, or **1** at different concentrations. Paclitaxel at 25 nM was

included as a positive MSA control. The percentage soluble or pelleted tubulin is given below each lane. Results are representative of 4 or more independent experiments. The percentage of tubulin relative to the total is given below each tubulin band

Table 4 CI values for persin/peloruside and persin/paclitaxel combinations in human 1A9 ovarian carcinoma cells

Persin (μM)	Peloruside A (nM)	CI \pm SEM	<i>n</i>	P value
5.0	5.0	0.5 \pm 0.1	5	0.0087
10.0	5.0	1.9 \pm 0.4	5	ns
10.0	10.0	2.0 \pm 0.3	5	ns
10.0	15.0	2.8 \pm 0.8	5	ns
15.0	5.0	0.6 \pm 0.1	5	0.0022
Persin (μM)	Paclitaxel (nM)	CI \pm SEM	<i>n</i>	P value
5.0	2.0	1.2 \pm 0.2	4	ns
5.0	5.0	1.3 \pm 0.2	4	ns
10.0	2.0	0.6 \pm 0.1	6	0.0012
10.0	5.0	0.7 \pm 0.1	6	0.0126
15.0	5.0	2.1 \pm 0.5	6	ns

Calculated values for the combination index (CI) are presented for persin/peloruside and persin/paclitaxel combinations. See Experimental Details for CI value calculation. Concentrations are given in μM for persin and nM for peloruside and paclitaxel. P values are calculated from a one-sample Student's *t*-test, and the number of biological replicates (*n*) is given in the table. ns = not significant. CI <1.0 = synergy; CI 1.0 = additivity; CI >1.0 = antagonism

the taxoid site [24], was unable to prevent Flutax-1 from binding, even when peloruside was present in excess (Fig. 4b).

Discussion

Persin, with its unique unsaturated, long-chain fatty acid-like polyketide structure and relative ease of extraction or total synthesis, shows potential for development as targeted therapy of breast cancer, given its specific and cumulative effect on mammary gland tissue [2, 9–11]. Its IC_{50} for growth inhibition is in the low micromolar range, and the aim of the present

study was to examine the structure-activity relationships of persin and seven of its analogs. In addition, we further characterized the microtubule-stabilizing activity of persin and selected analogs, as well as investigated their susceptibility to MDR and ability to synergize with other MSAs.

Bioactivity of persin analogs

The biological activity of persin, its saturated natural analog T-persin, and six synthetic analogs (Fig. 1) were tested for their activities in the leukemic cell line HL-60 and the ovarian cancer cell line 1A9. The total synthesis of these analogs has previously been described [22], together with their 24-h bioactivity in MCF-7 cells, and the activity of persin and T-persin across a range of cancer cell types (eight breast, two ovarian, and two prostate cancer cell lines). Persin was active in all but two of these cell types (breast cancer cell line MDA-MB-231 and the phenotypically normal epithelial breast cell line MCF-10A); whereas, conversely, T-persin was inactive in all but two of these cell types (breast cancer cell lines MCF-7 and T-47D) [22].

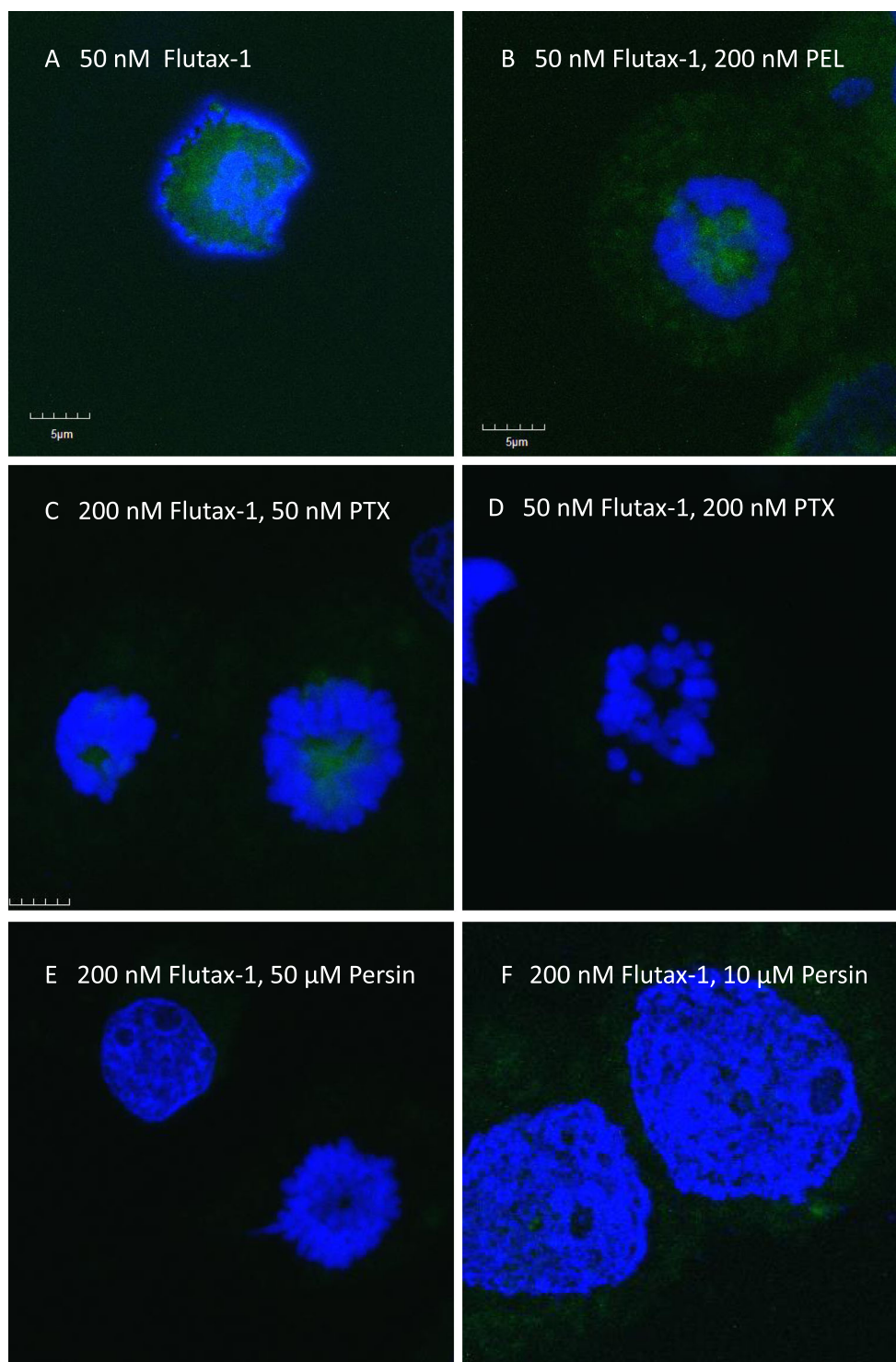
In the present study, the synthetic analogs displayed less potent anti-proliferative activities than persin and T-persin in HL-60 and 1A9 cells (Table 1), although it is notable that **1–4** retained single-digit, micromolar IC_{50} values in HL-60 cells. **1** was also tested in MCF-7 and MDA-MB-231 cell lines and, surprisingly, was more potent in the normally resistant MDA-MB-231 cells than in MCF-7. This contrasts with the relative inactivity ($\text{IC}_{50} > 39 \mu\text{M}$) of persin and T-persin in MDA-MB-231 in this (Table 1) and in the previous study [22] and demonstrates that a β -hydroxy ketone moiety is not the sole prerequisite for the biological activity of these compounds. While it is possible that the α,β -unsaturated system of **1** may impart Michael-accepting ability to this analog, the relative inactivity of **1** in MCF-7 cells [22] suggests that any such ability may not

Table 5 IC_{50} of persin and T-persin in mutant β -tubulin cells resistant to MSAs

Drugs	Cells						
	1A9	R1	L4	PTX-10	PTX-22	A8	B10
Persin	20.8 \pm 1.3	23.7 \pm 1.6	21.1 \pm 2.9	20.6 \pm 1.1	19.2 \pm 0.6	19.8 \pm 1.5	21.4 \pm 1.6
T-persin	20.7 \pm 1.6	22.7 \pm 1.5	21.4 \pm 1.4	20.7 \pm 3.3	20.4 \pm 1.6	19.9 \pm 2.5	22.3 \pm 0.2
PLA	15.9 \pm 0.8	101.0 \pm 5.5**	312.2 \pm 29.4**				
PTX	4.4 \pm 0.8			49.1 \pm 5.5*	88.1 \pm 4.5**		
IXA	5.1 \pm 1.2					62.6 \pm 1.5**	78.3 \pm 6.4*

The IC_{50} values of persin and T-persin are in μM and the IC_{50} values of peloruside A (PLA), paclitaxel (PTX), and ixabepilone (IXA) are in nM. 1A9 cells are the control cells with wild type β -tubulin. R1 cells have a mutation (A296T) in the laulimalide/peloruside binding site and show increased resistance to peloruside A. L4 cells have a mutation in the same binding site (R306H/C) and are resistant to both peloruside A and laulimalide. PTX-10 and PTX-22 cells have mutations in the taxoid binding site on β -tubulin (F270V and A364T, respectively) and are resistant to paclitaxel but not ixabepilone. A8 and B10 cells also have mutations in the taxoid binding site (T274I and A364T, respectively) and are resistant to ixabepilone. A8 also shows resistance to paclitaxel. * $P < 0.001$; ** $P < 0.0001$, Student's *t*-test comparing IC_{50} of a compound in the parental 1A9 cells with its IC_{50} in the mutant β -tubulin cells. Data are the average \pm SEM of 4 independent experiments

Fig. 4 Persin competition of Flutax binding. HL-60 cells in cell suspension were treated with different MSAs and Flutax-1 for 16 h, then centrifuged onto a glass slide in a Cytospin[®]3 centrifuge and mounted in DAPI plus Prolong Antifade. The green fluorescent staining of Flutax-1 bound to microtubules and blue fluorescent staining of DAPI bound to DNA were imaged in an Olympus FluoView FV1000 confocal microscope with a 100 \times objective. Image (a) shows the strong green fluorescence of Flutax-1 bound to the taxoid site, and image (b) is very similar. This indicates that, as expected, an excess of peloruside (PEL), an MSA that does not bind to the taxoid site, does not perturb the binding of Flutax-1 to this site. Image (c) shows that binding of excess Flutax-1 cannot be displaced by paclitaxel (PTX), but when paclitaxel is in excess, no green fluorescence can be seen (d). This shows that paclitaxel and Flutax-1 compete for the same binding site. Similarly, images (e) and (f) confirm that excess persin is able to compete with Flutax-1 for binding to the taxoid site. Results shown are representative of three independent experiments. The scale bar in panel A is 5 μ m, and all 6 images are at the same magnification



fully describe the activity of **1**. Moreover, a revival of interest in Michael acceptors as possible cancer treatments illustrates that molecules incorporating α,β -unsaturated systems may have utility in modern anti cancer drug development. This is exemplified by the development of 1,4-dienone derivatives of the natural product oridonin which are pro-apoptotic

in the resistant MDA-MB-231 cell line but relatively less toxic to normal cells [36], and the current Phase 1 trial of the 1,4-enone-containing PFKFB3 inhibitor ACT-PFK-158 for advanced solid malignancies [37].

Other structure-activity relationships evident from the data in Table 1 are that analogs **5** and **6** are clearly less potent than

persin and T-persin in both HL-60 and 1A9 cells, most likely due to the steric hindrance of an α -dimethyl group (**5**), and the lack of an extended sidechain (**6**). This was also seen previously in MCF-7 cells, in which the IC_{50} values of **5** and **6** were 29 μ M and >65 μ M, respectively [22]. The phenyl-substituted analogs **2**, **3**, and **4** retain reasonable potency in HL-60, but are relatively less efficacious in 1A9. It is noteworthy, however, that the diphenyl analog **3** is nearly as active as its monophenyl-substituted counterpart **2** in 1A9, whilst 4-bromophenyl compound **4** is significantly less potent than both **2** and **3** in this system. This differs from the trend observed for these compounds in MCF-7 cells in the previous study, in which **4** and **2** proved more potent than **3** [22], suggesting that different cancer types may be uniquely susceptible to different analogs of persin and T-persin, and further illustrates the non-essentiality of a β -hydroxy moiety for potency. Furthermore, the efficacy of analogs **1–4** in HL-60 show that persin and its close analogs may have particular utility against leukemias.

It is clear that the β -hydroxy ketone system of persin and T-persin is required for stabilization of the microtubule, since **1**, which lacks this moiety, is inactive with regard to both G_2M block (Table 2) and intracellular tubulin polymerization (Fig. 3). However, the fact that the growth-inhibitory activity of **1** against HL-60 cells is good, and against three other cell lines is moderate (Table 1), suggests that additional activity may hinge on the Michael-accepting ability of the α,β -unsaturated system of **1**. This may enable **1** to interfere with non-tubulin cellular pathways also targeted by persin, such as those mediated by acetyl-CoA carboxylase, a key enzyme in fatty acid biosynthesis that is inhibited by micromolar concentrations of persin [38].

Butt et al. [9] showed that persin promoted tubulin polymerization; however, the breast carcinoma cell line they used (MCF-7) has a high proportion of stabilized (polymerized) tubulin in the cell even in the absence of an MSA. Thus, the polymerized tubulin increased by only a small amount from 37% to 45% in the presence of persin [9]. To increase the chance of a greater increase in polymerized tubulin being visible, we chose to test intracellular tubulin polymerization in an ovarian carcinoma cell line (1A9) that has mostly soluble monomeric or dimeric tubulin in the absence of an MSA. As expected, persin and T-persin caused large changes in the relative proportions of soluble and polymerized tubulin in 1A9 cells, from 0% polymerized in the control to >56% polymerized at the highest concentrations tested (100 μ M) (Fig. 3). Butt et al. [9] had previously shown that persin caused microtubular bundling in MCF-7 cells (a sensitive cell line) but not in MDA-MB-231 cells (a resistant cell line), providing additional support for a microtubule-stabilization mode of action.

As **1** was the most cytotoxic of all six of the novel analogs (Table 1), it was selected for further investigation, and was

found to increase the proportion of cells in G_1 of the cell cycle and decreased the proportion in S phase (Fig. 1, Table 2). Although G_1 block is typical of compounds that inhibit DNA synthesis or interact with and block cyclin-dependent kinases (regulators of the cell cycle), there is little information available on other potential targets of persin and its derivatives, except the reported inhibition of acetyl-CoA carboxylase [38]. As suggested by Brooke et al. [22], persin may interfere with lipid metabolism; however, this hypothesis has yet to be tested. It is also important to note that persin becomes available only after its release in the gut from the ingested avocado matrix [2], and therefore studies carried out in cell lines may not be entirely representative of the true action of persin if such action is due to a metabolite formed in vivo. For example, a persin metabolite may cause the necrosis and apoptosis seen in the mammary epithelium; whereas, persin and some of its other metabolites may target tubulin, as shown by us and previously by Butt et al. [9]. The effects of persin on estrogen receptor signaling in mammary epithelium indicate persin may have wider efficacy and a distinct mechanism of action compared to other polyunsaturated acids since most polyunsaturated fatty acids, unlike persin, have no effect in estrogen receptor-negative cell lines [10].

Lack of susceptibility to MDR

In other studies, the metastatic breast cancer cell line MDA-MB-231 was shown to be highly resistant to persin, possibly because of a decreased level of Bim in the cells [9, 10]. The MSA paclitaxel is known to directly bind anti-apoptotic protein Bcl2 [39], which is down-regulated in paclitaxel-resistant cells [40]. The demonstrated resistance of MDA-MB-231 cells to persin and its analogs is consistent with the results presented in Table 1, with the IC_{50} for persin being 38 μ M in MDA-MB-231 cells, 7-fold higher than its IC_{50} in MCF-7 cells, and also higher than its IC_{50} in the non-breast cancer HL-60 and 1A9 cell lines. In the present study, we concentrated on two cancer cell lines that were not derived from breast cancers, a promyeloid leukemic cell line (HL-60) and an ovarian cancer cell line (1A9). A recent paper by Bonilla-Porras et al. [12] using avocado extracts demonstrated that a lymphoblastic leukemic Jurkat cell line was also highly susceptible to growth inhibition by the extracts, an effect that has also been seen in human oral epithelial cells [17, 18] and human T-cells [19]. Thus, in addition to the potential use of persin to treat breast cancer, especially estrogen receptor-negative, tamoxifen-resistant forms [9–11], it may also have application to other forms of cancers, including those currently targeted by paclitaxel and other MSAs. Furthermore, persin and T-persin are not affected by overexpression of the P-gp pump (Table 3); thus, tumors that have developed the MDR phenotype would remain sensitive to these compounds.

Synergy of persin with paclitaxel and peloruside A

Persin interacted synergistically with both paclitaxel and peloruside A in 1A9 ovarian carcinoma cells (Table 4), suggesting that persin or one of its analogs could sensitize cells to taxane chemotherapy, especially in tumors that have acquired resistance to the taxane drugs. The effective dose of persin (IC_{50}), however, is 1000-fold higher than that of paclitaxel, and this could present challenges from a clinical perspective. Other researchers have demonstrated potent synergistic activity of persin with 4-hydroxytamoxifen in both estrogen receptor-positive and -negative breast cancer cell lines [10, 11]. In addition, oleic and γ -linolenic acid (Fig. 1), fatty acids that are structurally related to persin, have positive effects in combination with paclitaxel in estrogen receptor-positive breast cancers [8], and γ -linolenic acid has also demonstrated synergy with the microtubule-destabilizing agent vinorelbine in a range of breast cancer cells [41] and is efficacious as a combination therapy with tamoxifen for estrogen receptor-positive breast cancer [15].

It is possible that persin may have an effect in breast epithelium unrelated to its effect on tubulin, enabling it to directly trigger apoptosis in mammary tissue [9]. In support of this, Roberts et al. [10] demonstrated that persin and 4-hydroxytamoxifen can synergise in their effects on the ceramide-mediated apoptotic pathway. This may be independent of microtubule interactions, since the pro-apoptotic synergy of persin and 4-hydroxytamoxifen appears to be mediated by endoplasmic reticulum stress [11].

Localisation of the binding site for persin on β -tubulin

Although the evidence is indirect, the synergy data suggested that if persin and T-persin act by directly binding to tubulin as proposed, their binding site may be unique and located on either α - or β -tubulin. However, as stated above, it is also possible that persin and T-persin can cause tubulin polymerization indirectly via a protein that associates with microtubules, or that they have secondary, non-microtubule targets. Evidence for the latter is seen by the fact that **1** retained similar anti-proliferative activity to persin in 1A9 cells, despite its inability to either block cells in G_2M of the cell cycle (Fig. 2, Table 2), or polymerize intracellular tubulin (Fig. 3). As discussed, the α,β -unsaturated system of **1** may also enable it to participate in Michael addition reactions, the utility of which in anti cancer drug development is currently being re-explored.

The studies in β -tubulin mutant cell lines resistant to other MSAs (Table 5) showed that both persin and T-persin retained their full activity in the mutant cell lines. Thus persin, or one of its analogs, may be useful in combination with other MSAs, as well as on its own, for a tumor that has developed resistance to current clinical MSAs. The lack of effect of a point mutation at

the taxoid binding site in tubulin on persin activity indicated that persin may not bind to the taxoid site or that persin may interact with the microtubule in a manner different to that exhibited by traditional MSAs. Although we tried to directly polymerize purified bovine tubulin in vitro using a standard protocol, we were, for reasons unclear, unsuccessful in our attempts. One possible cause may have been a high light-scattering background that we observed in the persin sample at $t=0$, suggesting possible non-specific precipitation of tubulin in the presence of persin. Another possible explanation is that the mechanism by which persin induces tubulin polymerization may not involve a direct interaction with the microtubule, but may occur via a binding interaction between persin and a microtubule-associated protein, or another key protein such as stathmin or dynein. To test this, we carried out a competition experiment and found that persin at high concentrations was able to displace a bound MSA (Flutax-1) from the microtubule, indicating that it must bind in the vicinity of the taxoid site on β -tubulin. Although this may seem to be inconsistent with our observation that mutations in β -tubulin at the taxoid site had no effect on persin activity, analogous results (i.e. two or more MSAs binding to the taxoid site but nevertheless having different susceptibilities to specific amino acid mutations at the taxoid site) have been previously described for paclitaxel, epothilone, and discodermolide [28, 42, 43]. In addition, two MSAs that are known to bind in the taxoid site, paclitaxel and discodermolide, have been shown to synergise with each other [44–46].

Conclusions

Persin has activity that is estrogen receptor-independent and is active against cancer cells that have an MDR phenotype; therefore, it has potential for treating refractory disease, an area in which many chemotherapeutics are currently failing. Evidence presented here suggests that persin binds to the taxoid site on β -tubulin and, based on the activity of analog **1**, may also have a secondary target in addition to the microtubule. Further studies investigating the tubulin-binding site interactions of persin, its possible secondary targets, and its structure-activity relationships would benefit its further characterization as a potential anticancer chemotherapeutic for use on its own or in combination with other anticancer drugs.

Acknowledgments This work was supported by grants from the Cancer Society of New Zealand, Wellington Medical Research Foundation (JJF, AK, JHM), the Joy McNicoll Postgraduate Research Award in Biomedical Science (JJF), and Victoria University of Wellington (JJF, AK, JHM). We thank Dr Paraskevi Giannakkakou for the 1A9 β -tubulin mutant cell lines, and Dr Peter Northcote and Dr Jonathan Singh for the supply of the natural product peloruside A.

Compliance with ethical standards

Conflict of interest The authors declare that they have no conflict of interest.

References

- Chang C-F, Isogai A, Kamikado T, Murakoshi S, Sakurai A, Tamura S (1975) Isolation and structure elucidation of growth inhibitors for silkworm larvae from avocado leaves. *Agric Biol Chem* 39:1167–1168
- Oelrichs PB, JNg JC, Seawright AA, Ward W, Schäffeler L, MacLeod JK (1995) Isolation and identification of a compound from avocado (*Persea americana*) leaves which causes necrosis of the acinar epithelium of the lactating mammary gland and the myocardium. *Nat Toxins* 3:344–349
- MacLeod JK, Schäffeler L (1995) A short enantioselective synthesis of a biologically active compound from *Persea americana*. *J Nat Prod* 58:1270–1273
- Prusky D, Keen NT, Sims JJ, Midland SL (1982) Possible involvement of an antifungal diene in the latency of *Colletotrichum gloeosporioides* on unripe avocado fruits. *Phytopathology* 72:1578–1582
- Rodriguez-Saona C, Millar JG, Maynard DF, Trumble JT (1998) Novel antifeedant and insecticidal compounds from avocado idioblast cell oil. *J Chem Ecol* 24:867–889
- Carman RM, Duffield AR, Handley PN, Karoli T (2000) 2-Hydroxy-4-oxohenicosan-1-yl acetate. Its presence in avocado and its simple chemistry. *Aust J Chem* 53:191–194
- Kingsbury JM (1964) *Poisonous Plants of the United States and Canada*. Prentice-Hall, Inc., Englewood Cliffs, 124
- Menéndez JA, Barbacid MD, Montero S, Sevilla E, Escrich E, Solanas M, Cortes-Funes H, Colomer R (2001) Effects of gamma-linolenic acid and oleic acid on paclitaxel cytotoxicity in human breast cancer cells. *Eur J Cancer* 37:402–413
- Butt AJ, Roberts CG, Seawright AA, Oelrichs PB, MacLeod JK, Liaw TYE, Kavallaris M, Somers-Edgar TJ, Lehrbach GM, Watts CK, Sutherland RL (2006) A novel plant toxin, persin, with in vivo activity in the mammary gland, induces Bim-dependent apoptosis in human breast cancer cells. *Mol Cancer Ther* 5:2300–2309
- Roberts CG, Gurisik E, Biden TJ, Sutherland RL, Butt AJ (2007) Synergistic cytotoxicity between tamoxifen and the plant toxin persin in human breast cancer cells is dependent on Bim expression and mediated by modulation of ceramide metabolism. *Mol Cancer Ther* 6:2777–2785
- McCloy RA, Shelley EJ, Roberts CG, Boslem E, Biden TJ, Nicholson RI, Gee JM, Sutherland RL, Musgrove EA, Burgess A, Butt AJ (2013) Role of endoplasmic reticulum stress induction by the plant toxin, persin, in overcoming resistance to the apoptotic effects of tamoxifen in human breast cancer cells. *Brit J Cancer* 109:3034–3041
- Bonilla-Porras AR, Salazar-Ospina A, Jimenez-Del-Rio M, Pereañez-Jimenez A, Velez-Pardo C (2014) Pro-apoptotic effect of *Persea americana* var. Hass (avocado) on Jurkat lymphoblastic leukemia cells. *Pharm Biol* 52:458–465
- Jordan MA, Wilson L (2004) Microtubules as a target for anticancer drugs. *Nat Rev Cancer* 4:253–265
- Haldar S, Chintapalli J, Croce CM (1996) Taxol induces Bcl-2 phosphorylation and death of prostate cancer cells. *Cancer Res* 56:1253–1255
- Kenny FS, Pinder SE, Ellis IO, Gee JM, Nicholson RL, Bryce RP, Robertson JF (2000) Gamma linolenic acid with tamoxifen as primary therapy in breast cancer. *Int J Cancer* 85:643–648
- Puthalakath H, Huang DC, O'Reilly LA, King SM, Strasser A (1999) The proapoptotic activity of the Bcl-2 family member Bim is regulated by interaction with the dynein motor complex. *Mol Cell* 3:287–296
- Ding H, Chin YW, Kinghorn AD, D'Ambrosio SM (2007) Chemopreventive characteristics of avocado fruit. *Semin Cancer Biol* 17:386–394
- Ding H, Han C, Guo D, Chin YW, Ding Y, Kinghorn AD, D'Ambrosio SM (2009) Selective induction of apoptosis of human oral cancer cell lines by avocado extracts via a ROS-mediated mechanism. *Nutr Cancer* 61:348–356
- Paul R, Kulkarni P, Ganesh N (2011) Avocado fruit (*Persea americana* Mill) exhibits chemo-protective potentiality against cyclophosphamide induced genotoxicity in human lymphocyte culture. *J Exp Ther Oncol* 9:221–230
- Lu H, Ouyang W, Huang C (2006) Inflammation, a key event in cancer development. *Mol Cancer Res* 4:221–233
- Rodriguez-Saona C, Millar JG, Trumble JT (1998) Isolation, identification, and biological activity of isopersin, a new compound from avocado idioblast oil cells. *J Nat Prod* 61:1168–1170
- Brooke DG, Shelley EJ, Roberts CG, Denny WA, Sutherland RL, Butt AJ (2011) Synthesis and in vitro evaluation of analogues of avocado-produced toxin (+)-(R)-persin in human breast cancer cells. *Bioorg Med Chem* 19:7033–7043
- Prota AE, Bargsten K, Zurwerra D, Field JJ, Díaz JF, Altmann K-H, Steinmetz MO (2013) Molecular mechanism of action of microtubule-stabilizing agents. *Science* 339:587–590
- Prota AE, Bargsten K, Northcote PT, Marsh M, Altmann K-H, Miller JH, Díaz JF, Steinmetz MO (2014) Structural basis of microtubule stabilization by laulimalide and peloruside A. *Angew Chem Int Ed* 53:1621–1625
- West LM, Northcote PT, Battershill CN (2000) Peloruside A: a potent cytotoxic macrolide isolated from the New Zealand marine sponge *Mycale* sp. *J Org Chem* 65:445–449
- Field JJ, Singh AJ, Kanakkanthara A, Halafih T, Northcote PT, Miller JH (2009) Microtubule-stabilizing activity of zampanolide, a potent macrolide isolated from the Tongan marine sponge *Cacospongia mycofijiensis*. *J Med Chem* 52:7328–7332
- Hood KA, West LM, Northcote PT, Berridge MV, Miller JH, Induction of apoptosis by the marine sponge (*Mycale*) metabolites, mycalamide A and pateamine. *Apoptosis* 6:207–219.
- Giannakakou P, Sackett DL, Kang YK, Zhan Z, Buters JTM, Fojo T, Poruchynsky MS (1997) Paclitaxel-resistant human ovarian cancer cells have mutant β -tubulins that exhibit impaired paclitaxel-driven polymerization. *J Biol Chem* 272:17118–17125
- Wilmes A, Bargh K, Kelly C, Northcote PT, Miller JH (2007) Peloruside A synergizes with other microtubule stabilizing agents in cultured cancer cell lines. *Mol Pharm* 4:269–280
- Wilmes A, O'Sullivan D, Chan A, Chandrasen C, Paterson I, Northcote PT, La Flamme AC, Miller JH (2011) Synergistic interactions between peloruside A and other microtubule-stabilizing and destabilizing agents in cultured human ovarian carcinoma cells and murine T cells. *Cancer Chemother Pharmacol* 68:117–126
- Field JJ, Calvo E, Northcote PT, Miller JH, Altmann K-H, Díaz JF (2013) Methods for studying microtubule binding site interactions: Zampanolide as a covalent binding agent. In Wilson L and Correia JJ (eds) *Methods in Cell Biology*, Vol 115: Microtubules In Vitro, 2nd Ed, Academic Press, Burlington, Chapter 19, pp. 303–325
- Lalande M (1990) A reversible arrest point in the late G₁ phase of the mammalian cell cycle. *Exp Cell Res* 186:332–339
- Kanakkanthara A, Wilmes A, O'Brate A, Escuin D, Chan A, Gjyrezi A, Crawford J, Rawson P, Kivell B, Northcote PT, Hamel

- E, Giannakakou P, Miller JH (2011) Peloruside- and laulimalide-resistant human ovarian carcinoma cells have β I-tubulin mutations and altered expression of β II- and β III-tubulin isotypes. *Mol Cancer Ther* 10:1419–1429
34. Giannakakou P, Gussio R, Nogales E, Downing KH, Zaharevitz D, Bollbuck B, Poy G, Sackett D, Nicolaou KC, Fojo T (2000) A common pharmacophore for epothilone and taxanes: molecular basis for drug resistance conferred by tubulin mutations in human cancer cells. *Proc Natl Acad Sci U S A* 97:2904–2909
 35. Gaitanos TN, Buey RM, Díaz JF, Northcote PT, Teesdale-Spittle P, Andreu JM, Miller JH (2004) Peloruside A does not bind to the taxoid site on β -tubulin and retains its activity in multidrug resistant cell lines. *Cancer Res* 64:5063–5067
 36. Ding C, Zhang Y, Chen H, Yang Z, Wild C, Ye N, Ester CD, Xiong A, White MA, Shen Q, Zhou J (2013) Oridonin ring A-based diverse constructions of enone functionality: identification of novel dienone analogues effective for highly aggressive breast cancer by inducing apoptosis. *J Med Chem* 56:8814–8825
 37. Phase I safety study of ACT-PFK-158, 2HCl in patients with advanced solid malignancies: <https://clinicaltrials.gov/ct2/show/NCT02044861> Accessed 18 Dec 2015
 38. Hashimura H, Ueda C, Kawabata J, Kasai T (2001) Acetyl-CoA carboxylase inhibitors from avocado (*Persea americana* Mill) fruits. *Biosci Biotechnol Biochem* 65:1656–1658
 39. Ferlini C, Cicchillitti L, Raspaglio G, Bartollino S, Cimitan S, Bertucci C, Mozzetti S, Gallo D, Persico M, Fattorusso C, Campiani G, Scambia G (2009) Paclitaxel directly binds to Bcl-2 and functionally mimics activity of Nur77. *Cancer Res* 69:6906–6914
 40. Ferlini C, Raspaglio G, Mozzetti S, Martinelli E, Ferrandina G, Gallo D, Riva A, Bombardelli E, Morazzoni P, Scambia G (2003) Bcl-2 downregulation is a novel mechanism of paclitaxel resistance. *P. Am. Assoc Cancer Res* 44:1104–1104
 41. Menéndez JA, Roper S, del Barbadid MM, Montero S, Solanas M, Escrich E, Cortés-Funes H, Colomer R (2002) Synergistic interaction between vinorelbine and gamma-linolenic acid in breast cancer cells. *Breast Cancer Res Treat* 72:203–219
 42. Kowalski RJ, Giannakakou P, Gunasekera P, Longley RE, Day BW, Hamel E (1997) The microtubule-stabilizing agent discodermolide competitively inhibits the binding of paclitaxel (Taxol) to tubulin polymers, enhances tubulin nucleation reactions more potently than paclitaxel, and inhibits the growth of paclitaxel-resistant cells. *Mol Pharmacol* 52:613–622
 43. He L, Yang C-PH, Horwitz SB (2001) Mutations in β -tubulin map to domains involved in regulation of microtubule stability in epothilone-resistant cell lines. *Mol Cancer Ther* 1:3–10
 44. Martello LA, McDaid HM, Regl DL, Yang CP, Meng D, Pettus TR, Kaufman MD, Arimoto H, Danishefsky SJ, Smith AB 3rd, Horwitz SB (2000) Taxol and discodermolide represent a synergistic drug combination in human carcinoma cell lines. *Clin Cancer Res* 6:1978–1987
 45. Giannakakou P (2000) Fojo T (2000) Discodermolide: just another microtubule-stabilizing agent? No! A lesson in synergy. *Clin Cancer Res* 6:1613–1615
 46. Honore S, Kamath K, Braguer D, Horwitz SB, Wilson L, Briand C, Jordan MA (2004) Synergistic suppression of microtubule dynamics by discodermolide and paclitaxel in non-small cell lung carcinoma cells. *Cancer Res* 64:4957–4964